Available online at www.sciencedirect.com
ScienceDirect
Energy Procedia 48 (2014) 618 – 627
Energy Procedia

SHC 2013, International Conference on Solar Heating and Cooling for Buildings and Industry
September 23-25, 2013, Freiburg, Germany

Spectrally splitting hybrid photovoltaic/thermal receiver design for a linear concentrator

Ahmad Mojiri[a], Cameron Stanley[a], Gary Rosengarten[a]*

[a]*School of Aerospace, Mechanical and Manufacturing Engineering, RMIT University, 115 Queensberry Street, Carlton, Melbourne 3053, Australia*

Abstract

A new spectrally splitting photovoltaic-thermal hybrid receiver has been proposed and optimised for use in a linear concentrator with 10 to 20 suns concentration level. This hybrid system can produce high temperature thermal energy along with electrical output. Since photovoltaic cells cannot operate efficiently at high temperatures, they have been thermally decoupled from the thermal sub-module through spectral beam splitting, to avoid excessive heating of the cells. The proposed configuration incorporates a combination of dichroic filtering and selective volumetric absorption to divide the spectrum between the cells and the thermal sub-modules. The optics of the system has been studied using ray tracing and its performance has been compared against an ideal spectrally splitting system showing promising results.

Selection and peer review by the scientific conference committee of SHC 2013 under responsibility of PSE AG

Keywords: Solar hybrid receiver; photovoltaic; thermal; spectral splitting; concentrating

1. Introduction

Photovoltaic/thermal hybrid solar collectors can produce heat and electricity at the same time and help to increase the sunlight collection efficiency in solar collectors. The working principle of such collectors is based on the fact that just a fraction of the sunlight (e.g. 14-20% in silicon solar cells) is converted to electricity through the photovoltaic effect. The rest of the energy is dissipated as heat in the cell. In traditional hybrid collectors, the PV

* Corresponding author. Tel.: +61 3 9925 8020.
E-mail address: gary.rosengarten@rmit.edu.au

Selection and peer review by the scientific conference committee of SHC 2013 under responsibility of PSE AG
doi:10.1016/j.egypro.2014.02.072

cells are thermally coupled to a heat transfer fluid that absorbs the generated heat and delivers useful thermal output for low temperature applications. The maximum temperature of such devices is limited by the recommended operating temperature of the cells which is generally 80 ℃ for silicon solar cells.

By thermally decoupling the cells from the heat transfer fluid, the thermal output temperature of such hybrid collectors can increase independently from the cell temperatures. To do so, the sunlight is spectrally split into different wavelength bands. The most suitable band is directed to the cells and the rest of the spectrum is converted into heat in a parallel high-temperature thermal receiver [1, 2]. Crisostomo et al [3] suggested that the suitable spectral band for silicon solar cells is approximately 700-1100 nm. By separating this spectral band from the rest of the spectrum and directing it to silicon cells, high electrical conversion efficiencies such as 30% (with respect to the total solar energy in this band) can be achieved. Two methods for spectrally splitting of the sunlight have been proposed: (1) selective absorption [4] and (2) wave interference filtering [5].

Generally, in the selective absorption method a heat transfer liquid that is transparent to the desired wavelengths for PV cells is located in front of them letting those wavelengths be transmitted to the cells. The liquid is highly absorbing in the rest of the spectrum and absorbs it as heat. However, matching the spectral absorption/transmission properties of liquids for this purpose is challenging. Alternatively, wave interference filters provide a high degree of flexibility in the spectral modification of light. One main category of interference filters is thin film optical filters, which are formed from a number of layers of at least two transparent materials with distinct refractive indices deposited on a substrate [6]. Theoretically, by changing the number of layers and their thicknesses, any reflection/transmission curve can be attained. Despite the flexibility in their design performance, a challenge of using these filters in solar energy applications is their increased complexity and relatively expensive fabrication processes. This paper introduces a novel spectrally splitting hybrid receiver for a rooftop linear micro-concentrator (LMC) combining the interference technology with direct absorption method to provide a simpler spectral splitter.

Nomenclature

LMC	linear micro concentrator
PV	photovoltaic
sr	steradian
λ	wavelength (*nm*)
I	irradiance (W/m^2)
I_λ	spectral irradiance ($W/m^2/nm$)
θ_{mean}	power weighted mean angle of incidence (*degrees*)
θ	polar angle (*radians*)
ϕ	azimuthal angle (*radians*)
$I_{(\theta,\phi)}$	angular flux (W/sr)
TiO_2	titanium dioxide
SiO_2	silicon dioxide
H	quarter wavelength-thick layer of TiO_2
L	quarter wavelength-thick layer of SiO_2
T_λ	spectral transmissivity
T	transmissivity
d	path length (m)
k	absorption index

2. Design description

In the current paper, "hybrid collector" refers to the combination of a rooftop linear micro-concentrator (LMC) and the hybrid receiver installed at its focal axis. The LMC generates up to 20 suns of average concentration level to produce high temperature heat as well as electricity. A ray tracing simulation of the LMC has been carried out to estimate the flux distribution at its focal axis in order to optimise the geometry of the proposed receiver based on the (1) spatial, (2) angular, and (3) spectral distribution of the incoming irradiance.

2.1. The rooftop linear micro-concentrator (LMC)

The LMC is a one-axis solar tracking linear concentrator developed and commercialised by Chromasun [7, 8]. It comprises of two sets of Fresnel reflectors, each set with 10 curved mirrors, encapsulated inside a glass canopy. The mirrors are controlled by a tracking system to focus the sunlight on a focal axis 25cm above the mirror plane. The whole box of the LMC is 3.3m long, 1.2m wide and 0.3m high. Figure 1 shows the geometry of the LMC. Figure 1c shows a cross section of the LMC along its longitudinal axis, including the solar rays, when the incident angle on the LMC is 90 degrees. Figure 1d is a schematic of the proposed hybrid receiver and will be discussed in detail below.

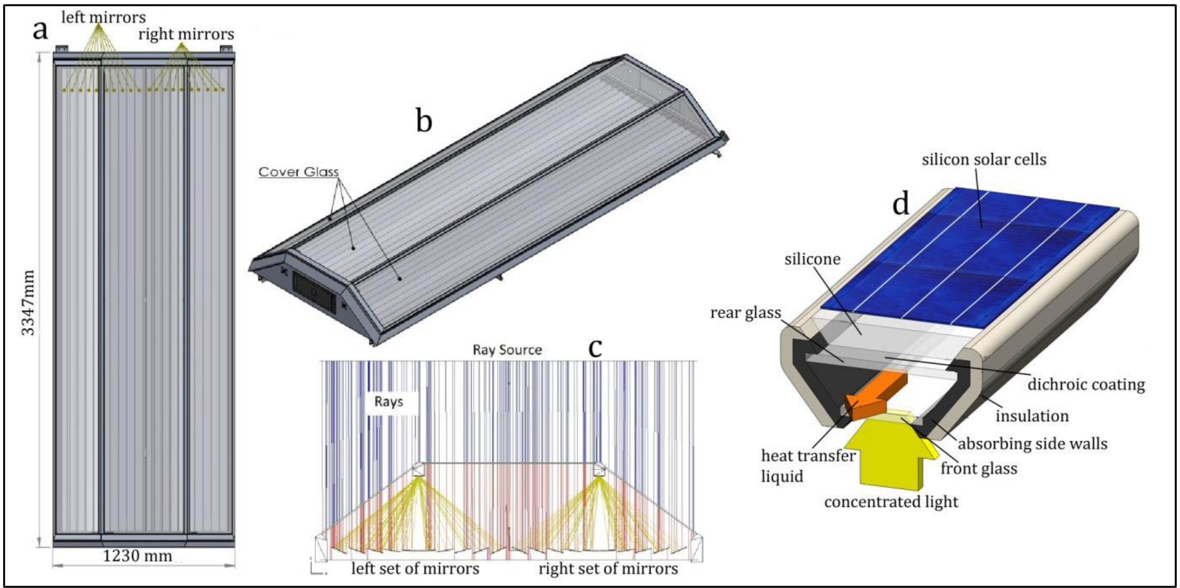

Figure 1, schematic of the collector (a) LMC top view; (b) LMC perspective; (c) cross section of LMC; (d) the hybrid receiver

2.2. The hybrid receiver design

The proposed hybrid receiver consists of a high temperature liquid channel coupled to crystalline silicon (Si) cells. The overall configuration of the receiver is presented in Figure 1d. Concentrated light propagates in the upward direction and enters the receiver through the front glass. Light passes through this highly transparent glass and enters the semi-transparent liquid flowing inside the channel. This liquid acts as a high temperature heat transfer fluid as well as a spectral filter absorbing the infra-red region of the spectrum (above 1100nm) [4]. Potential candidate heat transfer liquids for temperatures above $100^{o}C$ include pressurised water, ethylene glycol, and propylene glycol [9].

Shorter wavelengths are transmitted through the liquid and the highly transparent rear glass with only minor attenuation, and strike the dichroic coating at the top surface of the rear glass (see Figure 1d). This coating acts as a long pass filter, reflecting the wavelengths shorter than 700nm and transmitting the remainder of the spectrum. The reflected and transmitted rays are absorbed by the absorbing side walls (as heat) and the Si cells respectively. The outside of the absorbing side walls are thermally insulated in order to minimise the heat loss from the thermal receiver. Consequently, the spectral band reaching the PV cells will be in the 700-1100nm range with the rest of the spectrum being absorbed either directly by the liquid or by the absorbing side walls, which is then transferred into the liquid via convective heat transfer.

The geometrical and optical design of the hybrid receiver is driven by the spatial, angular, and spectral properties of the concentrated light at the focal axis of the LMC. For this reason a ray tracing model has been used as the building block of the receiver design, allowing the extraction of this data and parameter optimisation, and will be presented in the following section.

3. Methods

This section describes the optical modeling of the above system including the LMC and the hybrid receiver. The orientation of the LMC, sun angle, shadows from the structure, and the geometrical arrangement of the mirrors can affect the spatial and angular distribution of light at the focal region. In addition to this, the spectral distribution of the sunlight at the focal region of the LMC is different from the original solar spectrum because the sunlight passes through the cover glass and gets reflected by the mirrors before reaching the receiver (see Figure 1); both of these components have wavelength dependent optical properties (i.e. reflectivity and transmissivity).

3.1. Optical modeling of the LMC

Unlike parabolic troughs, the LMC has a relatively more complicated concentrating mechanism that comprises of a number of discrete narrow cylindrically curved mirrors controlled by a single axis tracking systems. Hence, ray tracing method using ZEMAX optical software [10] has been used to investigate the optics of the systems. In this modeling, the sun was defined as a radial source at infinity. Since the sun is not a point source (because of its significant size compared to its distance from the earth) a sun half angle of 0.27° [11] was incorporated in the model. This can influence the radiation distribution in the focal region of solar concentrators.

In order to model a spectral beam splitting receiver properly, the spectrum of the sunlight was defined in accordance with the reference air mass 1.5 solar spectrum [12]. The total power of the ray source in ZEMAX was calculated through the below equation:

$$I\left(W/_{m^2} \right) = \int_{280nm}^{4000nm} I_\lambda d\lambda \tag{1}$$

In the above equation, I is the irradiance of the light source, I_λ is the spectral irradiance ($W/m^2/nm$) of the beam component of air mass 1.5 solar spectrum and λ is wavelength in nm. The reason why only the direct beam component of the spectrum has been used here is that Fresnel concentrators such as the LMC are not capable of concentrating the diffuse component of the sunlight. The above integration has been carried out numerically resulting in 900 W/m^2 as the source power.

After defining the geometries, light sources, and optical properties of materials in ZEMAX, a 40 mm long section of the receiver was included in the final ray tracing simulation, as there is no longitudinal variation in the flux. Convergence of the model was checked and it was found that increasing the number of rays above 2 million resulted in variations of less than 0.1% in the amount of energy absorbed by different sub components such as water, PV cells, and side walls.

3.2. The spatial and angular flux distribution upon the receiver

Figure 2 shows the distribution of the incoming power on the bottom face of the front glass (aperture area of the receiver). These results exclude the effect of tracking errors and non-ideal surface properties of the mirrors; any variation in these factors can change the spatial distribution of the flux at the focal point of any solar concentrator. For example including tracking errors and mirror surface inaccuracies in the optical modeling will cause a wider focal spot (lower solar concentration).

Figure 2b shows the angular distribution of the impinging flux upon the receiver. The distribution should be taken into account in designing the hybrid receiver because:

- The light rays should not intercept the side absorbing walls before hitting the dichroic coating on top of the rear glass; otherwise they will be absorbed as heat without being split into suitable spectral bands.
- The reflection/transmission characteristics of dichroic filters deviate from the desired case by changing the incident angle of the incoming light [5]. This is because of variation in the optical path of the rays through the layers.

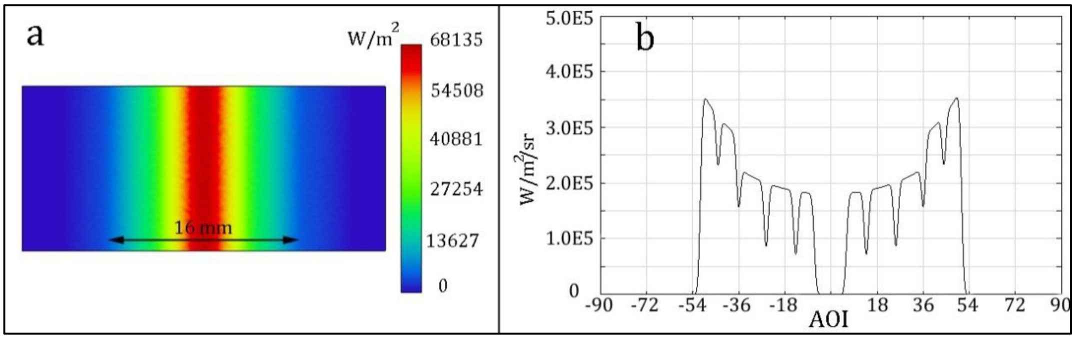

Figure 2, (a) the irradiance distribution (W/m^2) and (b) the angular distribution of the flux on the aperture of the receiver

The first issue can be addresses by setting the absorber side walls orientation at such angle that keeps them out of the incoming light propagation path. The second issue can be mitigated by using the power weighted mean angle of incidence in designing the thin film dichroic coating [13]. This has been explained in the next two sections.

3.3. The dichroic filter design

The materials considered here for fabricating the dichroic coating are SiO_2 and TiO_2. This pair of materials has been widely used in designing dichroic coatings and has been extensively investigated by researchers [6]. The first step in designing the required coating is calculating the power weighted mean angle of incidence on the top face of the rear glass. This can be calculated as below:

$$\theta_{mean} = \frac{\int_0^{\pi}\int_0^{\frac{\pi}{2}} \theta . I_{(\theta,\phi)} . \sin\theta . d\theta . d\phi}{\int_0^{\pi}\int_0^{\frac{\pi}{2}} I_{(\theta,\phi)} . \sin\theta . d\theta . d\phi} \tag{2}$$

In the above equation, $I_{(\theta,\phi)}$ is the angular power (*W/sr*) on the top face of the rear glass which is the location of the dichroic coating. θ and ϕ are respectively polar and azimuthal angle as defined in spherical coordinates. $I_{(\theta,\phi)}$ was extracted from ray tracing results through some mathematical modifications that have not been mentioned here. θ_{mean} is the power weighted mean angle of incidence that is equal to 18.6 degrees for this specific concentrator when the sun is exactly above the collector, normal to its aperture area.

The dichroic coating, which is a long pass filter, was designed according to the above mean angle of incidence when the front and back medium of the coating was defined to be glass and silicone respectively. It has been shown that for long pass filters on glass substrates a [(*H/2*) *L* (*H/2*)] stack formula creates satisfactory results. In this formula *H* and *L* are quarter wavelength-thick layers of high and low refractive index materials respectively [6]. In the current design TiO_2 and SiO_2 are the high and low refractive index materials. 550 nm was taken as the reference wavelength. The initial stack was defined as below that includes 14 sets of the above combination:

$$\left(0.5H\ L\ 0.5H\right)^{14} \tag{3}$$

The above stack was refined by varying the thickness of individual layers to match the target reflection/transmission curve. The refinement has been carried out using an open source thin film filter design code, “Openfilters” [14]. The results have been shown in Figure 3. The refined coating is: *H*(59)*L*(51) *H*(83)*L*(74) *H*(78)*L*(69) *H*(70)*L*(67) *H*(78)*L*(123) *H*(28)*L*(144) *H*(69)*L*(45) *H*(256)*L*(96) *H*(45)*L*(92) *H*(48)*L*(70) *H*(26)*L*(95) *H*(49)*L*(84) *H*(40) with the total thickness of 1948nm. The numbers in brackets in this stack formula are absolute thicknesses of the corresponding layers in nm.

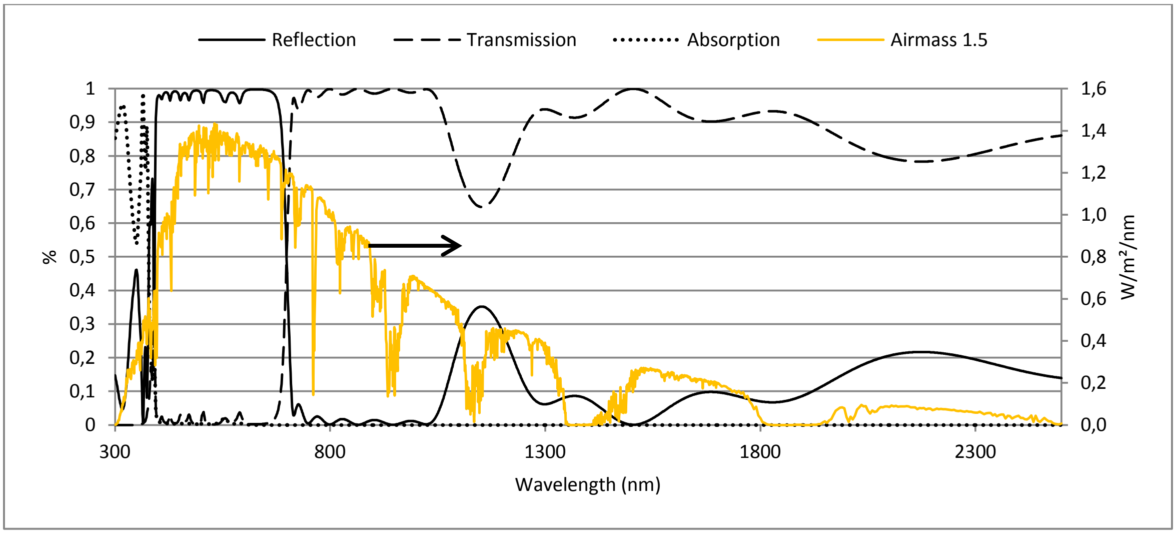

Figure 3, the spectral characteristics of the dichroic coating along with the air mass 1.5 solar spectrum

The average transmission of the coating over the solar spectrum between two wavelengths, λ_1 and λ_2, can be calculated as below:

$$T_{\lambda_1-\lambda_2} = \frac{\int_{\lambda_1}^{\lambda_2} I_\lambda . T_\lambda . d\lambda}{\int_{\lambda_1}^{\lambda_2} I_\lambda . d\lambda} \tag{4}$$

In this equation, T_λ is the spectral transmissivity at wavelength λ and I_λ is the spectral irradiance of the solar spectrum. This equation has been used in the next sections to evaluate the performance of the filters.

3.4. Optical properties of the heat transfer liquids

Three potential heat transfer liquids with suitable optical properties for such a design are: water, propylene glycol, and ethylene glycol. The optical properties of these liquids are presented in Figure 4. The transmission of the liquids has been calculated from the absorption index using Beer’s law as presented in equation (5).

$$T = e^{\frac{-4\pi k d}{\lambda}} \tag{5}$$

In this equation d is path length and k is absorption index. The absorption edge of water occurs closer to the desired cut-off wavelength (1100 nm) compared to the other two materials. In addition to this, water is the cheapest fluid and doesn't suffer from optical degradation under thermal cycling or direct solar radiation. For these reasons water has been chosen as the heat transfer fluid for the current work. Despite this, consideration of the elevated operating temperature of the thermal absorber may justify using propylene glycol or ethylene glycol that have higher boiling temperatures than water, eliminating the need for channel pressurisation.

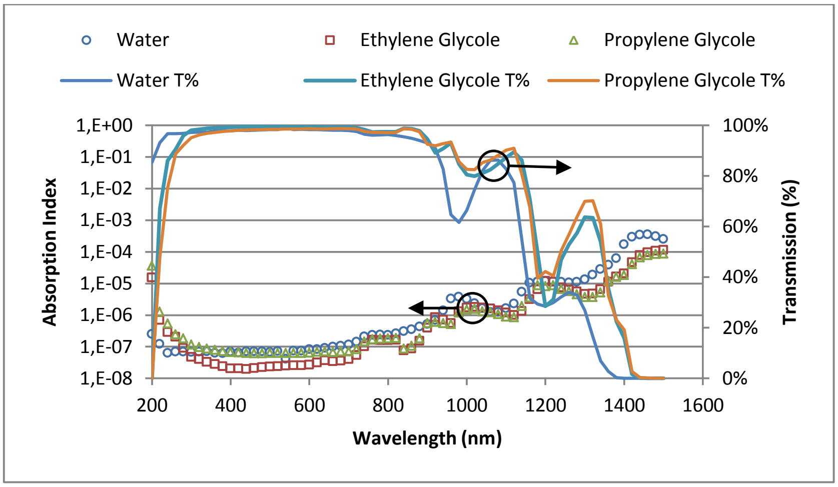

Figure 4, absorption index and transmission of water ethylene glycol, and propylene glycol

4. Results and discussion

The optical analysis of the receiver has been schematically presented in Figure 5. Figure 5a shows the distribution of the impinging power upon each element inside the receiver. It can be seen that light is partially reflected toward the side walls after hitting the top face of the rear glass (presented by a solid line underneath the silicone layer), which is coated with the dichroic layer. A portion of the light hitting the dichroic coating is transmitted all the way through the silicone layer, with insignificant attenuation, to the silicon cells. Since the side absorbers have been assumed to be 100% absorbing, no reflection from their surface has been observed. The maximum optical concentration level is at the entrance of the receiver just below the front glass. This is desirable as it allows minimization of the required aperture area, which, additionally, reduces the thermal losses from the receiver along with resulting in a more compact design.

Figure 5b shows the energy absorbed by water along the light transmission path. It can be seen that the majority of absorption occurs in the layer of water immediately adjacent to the front glass (approximately 1mm); this is due to high absorption of water for wavelengths longer than 1200nm. Some energy corresponding to the 900-1200nm band is absorbed further into the water because of water's moderate absorption in this band. It should be noted that the power reported in these contours are Watts per meter length of the receiver, assuming that there is no variation in the longitudinal direction; an acceptable assumption for cylindrical concentrators ignoring shadows.

The solar weighted transmission of the dichroic filter has been calculated using equation (4). This result, accompanied by the transmission values for the liquid channel including the water layer, front and rear glass panels are presented in Table 1. It can be seen that the dichroic filter is highly reflective in the spectral band shorter than 700nm and is highly transparent in the desired band between 700nm and 1100nm. The high transmission of the dichroic filter (85.7%) beyond 1100 nm is not an issue provided the transmission of the liquid channel in the same range is low; the liquid channel has 11.2% transmission in this range. This value is determined using the intrinsic absorption coefficient of the liquid and its thickness.

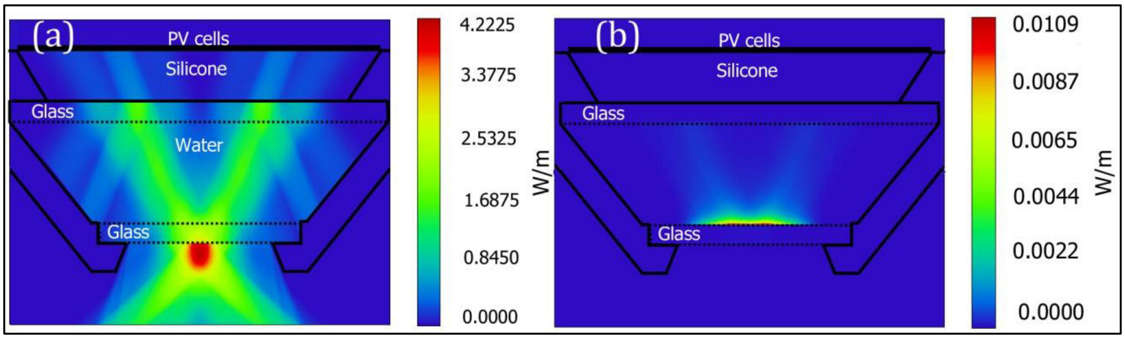

Figure 5, ray tracing of the volumetric receiver; (a) impinging power at each point; (b) power absorbed by water

Table 1, Transmission properties of the dichroic filters and the liquid channel

	Spectral band	Transmission
Dichroic filter		
	280nm – 700 nm	2.6%
	700nm – 1100 nm	96.5%
	1100 nm – 4000 nm	85.7%
Liquid channel		
	280nm – 700 nm	93.9%
	700nm – 1100 nm	83.2%
	1100 nm – 4000 nm	11.2%

Owing to the angle of incidence, the majority of the light reflected from the rear glass is absorbed by the side walls. However 6% of the total power incident upon the front glass is reflected by the dichroic coating and passes back through the front glass without being absorbed by the side walls. This is an optical loss mechanism of the systems. The other optical loss occurs at the bottom face of the front glass through Fresnel reflection which is equates to 6.2%. Hence the total reflection loss from the receiver is equal to 12.2%. An overall energy balance of the receiver is presented in Table 2.

Table 2, Energy balance of the receiver

Component	%
Absorbed by the front glass	0.2
Absorbed by water	23.1
Absorbed by the rear glass	0.0
Absorbed by the side walls	33
Absorbed by the PV cells	31.5
Reflected by the whole receiver	12.2

As it can be seen in this table, 31.5% of the energy hitting the front glass is directed to the silicon cells whereas 53.1% is absorbed as heat by the side walls and volumetric absorption in water. The spectral distribution of the bands absorbed by each component, especially by the PV cells, is the main concern. The corresponding spectral distributions have been presented in Figure 6. Figure 6a presents the spectral distribution of the light at the entrance of the receiver before any spectral attenuation. It is close to the solar spectrum. Figure 6b shows the spectral distribution of the reflected missed rays. It is a combination of the Fresnel reflection from the front glass and the geometrical optical losses due to missing a portion of the light reflected from the dichroic coating. Figure 6c shows the spectral band corresponding to the energy absorbed by the side walls and is primarily in the spectral band <700nm. There is some energy absorbed in wavelengths close to 1100nm that is due to the reflection side lobe of the dichroic coating at this wavelength (see Figure 3). The spectral distribution of the power absorbed by the silicon cells is presented in Figure 6d. The majority of this power is in the 700-1100nm band however some radiation with wavelengths between 1100 and 1300 nm also reachs the cells. This is due to the non-ideality of the filter around1100 nm that relies on the optical absorption properties of water.

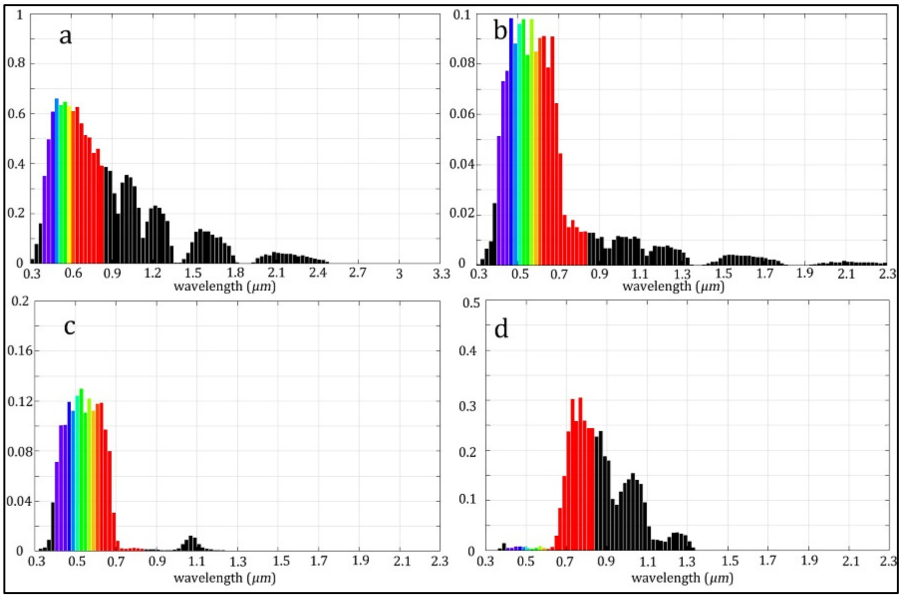

Figure 6, spectral distribution of (a) the impinging power upon the front glass; (b) reflected missed rays; (c) absorbed by the side walls; (d) absorbed by the PV cells; in all these figures the vertical axis has arbitrary units but with comparable values

Table 3 compares the spectral performance of the proposed spectral splitter against an ideal one. In the ideal case 100% of the power directed to silicon cells is within the 700-1100nm band compared to 87.8% for the proposed design. Additionally, 5.8% and 6.4% of the power reaching the PV are <700nm and >1100nm wavelength bands respectively and are not suitable for silicon cells. Considering these results the filter and receiver design presented within this work produces a good overall performance.

Table 3, Comparing the proposed filter performance against the ideal filter

Spectral band	**Percentage**	**Ideal percentage**	**Comment**
λ < 700 nm	5.8%	0%	Not desirable range
700 nm < λ < 1100 nm	87.8%	100%	Desirable range
λ > 1100 nm	6.4%	0%	Not desirable range
Total amount of energy on the receiver	356.5 (W/m)		
Total amount of energy absorbed by PV	112.5 (W/m)		

5. Conclusion

This article presents a new type spectral beam splitting hybrid solar receiver which demonstrates the potential for utilising a combination of dichroic filters with direct absorbing liquids for efficiently filtering of the incident sunlight. For the current work, receiver geometry was optimised for Chromasun's linear micro concentrator; however it can be optimised for other geometries and types of concentrators such as parabolic troughs. The results from optical modeling showed that the receiver is capable of directing 31.5% of the solar spectrum to the PV cells; 87.7% of this energy is within the desired range of 700nm -1100nm band. The rest of the solar spectrum is absorbed by the liquid channel and is converted to heat. The high temperature heat transfer fluid has been decoupled from the PV cell such that the maximum temperature of the thermal absorber is not limited by the cell operating temperature.

Acknowledgements

The authors would like to thank the University of RMIT for hosting this research. The authors would also like to thank the Australian Solar Institute and the Australian government for supporting this work and for providing a fellowship to Ahmad Mojiri.

References

[1] A.G. Imenes, D.R. Mills, Spectral beam splitting technology for increased conversion efficiency in solar concentrating systems: a review, Solar Energy Materials and Solar Cells, 84 (2004) 19-69.
[2] A. Mojiri, R. Taylor, E. Thomsen, G. Rosengarten, Spectral beam splitting for efficient conversion of solar energy—A review, Renewable and Sustainable Energy Reviews, 28 (2013) 654-663.
[3] F. Crisostomo, R.A. Taylor, A. Mojiri, E.R. Hawkes, D. Surjadi, G. Rosengarten, Beam Splitting Ssystem for the Development of a Concentrating Linear Fresenl Solar Hybrid PV/T Collector, in: Proceedings of the ASME 2013 Summer Heat Transfer Conference, Minneapolis, MN, USA, 2013.
[4] M.A.C. Chendo, M.R. Jacobson, D.E. Osborn, Liquid and thin-film filters for hybrid solar energy conversion systems, Solar & Wind Technology, 4 (1987) 131-138.
[5] M. Peters, J.C. Goldschmidt, P. Löper, B. Groß, J. Üpping, F. Dimroth, R. Wehrspohn, B. Bläsi, Spectrally-Selective Photonic Structures for PV Applications, Energies, 3 (2010) 171-193.
[6] H.A. Macleod, Thin-Film Optical Filters, 4th ed., CRC Press, United States of America, 2010.
[7] V. Everett, D. Walter, J. Harvey, M. Vivar, R. Van Scheppingen, S. Surve, A. Blakers, P. Le Lievre, M. Greaves, A. Tanner, A closed loop tracking system for a linear Fresnel hybrid PV/thermal micro-concentrator system, in: 25th European Photovoltaic Solar Energy Conference and Exhibition (25th EU PVSEC)/5th World Conference on Photovoltaic Energy Conversion (WCPEC-5), Valencia (Spain), 2010, pp. 1063-1065.
[8] T. Sultana, G.L. Morrison, G. Rosengarten, Thermal performance of a novel rooftop solar micro-concentrating collector, Solar Energy, 86 (2012) 1992-2000.
[9] T.P. Otanicar, P.E. Phelan, J.S. Golden, Optical properties of liquids for direct absorption solar thermal energy systems, Solar Energy, 83 (2009) 969-977.
[10] RadiantZemax, ZEMAX, in, http://radiantzemax.com/, 2012.
[11] S. Jiang, P. Hu, S. Mo, Z. Chen, Optical modeling for a two-stage parabolic trough concentrating photovoltaic/thermal system using spectral beam splitting technology, Solar Energy Materials and Solar Cells, 94 (2010) 1686-1696.
[12] N.R.E.L. (NREL), Reference Solar Spectral Irradiance: Air Mass 1.5, in, http://rredc.nrel.gov/solar/spectra/am1.5/, 2012.
[13] A.G. Imenes, D. Buie, D.R. Mills, P. Schramek, S.G. Bosi, A new strategy for improved spectral performance in solar power plants, Solar Energy, 80 (2006) 1263-1269.
[14] S. Larouche, L. Martinu, OpenFilters: open-source software for the design, optimization, and synthesis of optical filters, Appl. Opt., 47 (2008) C219-C230.